Supplemental Figure S1. RAD51 Cys319 has reactive nucleophilic characteristics

A

$$CysSH \rightleftharpoons CysS^- + H^+ \qquad \text{Eq. 1}$$

$$K_a = \frac{[H^+][CysS^-]}{[CysSH]} \qquad \text{Eq. 2}$$

$$pK_a = -\log K_a$$

$$pH = pK_a + \log \frac{[CysS^-]}{[CysSH]} \qquad \text{Eq. 3}$$

$$10^{(pK_a - pH)} = \frac{[CysS^-]}{[CysSH]}$$

B

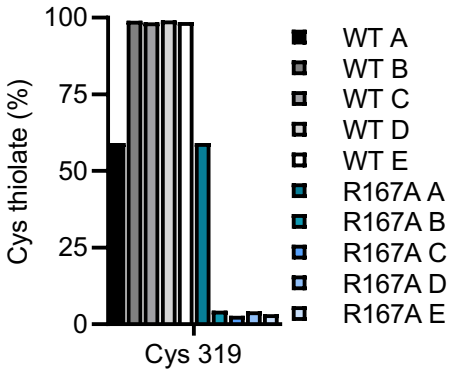

C

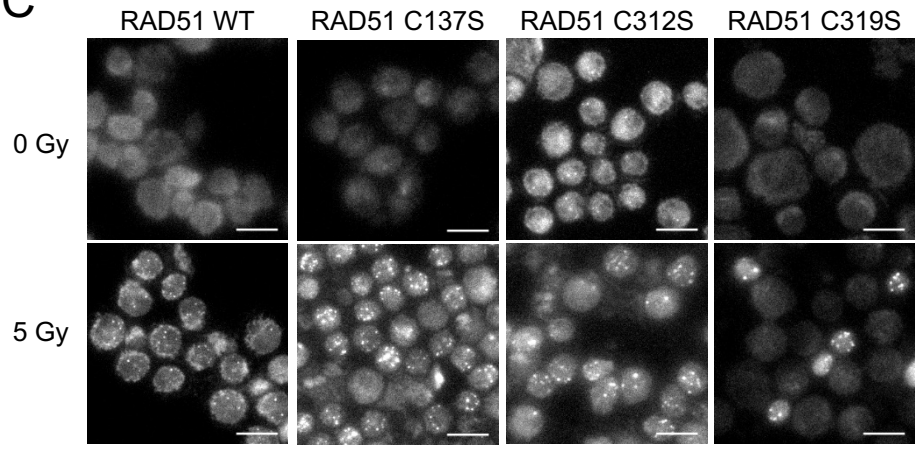

Supplemental Figure S1. RAD51 Cys319 has reactive nucleophilic characteristics. (*A*) Equations for deprotonation of cysteine (Eq. 1), the acid dissociation constant of cysteine K_a, with $[H^+]$, $[CysS^-]$ and [CysSH] at equilibrium concentrations (Eq. 2) and the Henderson-Hasselbalch (Eq. 3). (*B*) Cys thiolate levels were calculated using pKa values determined by PropKa from the Cryo-EM structure of human RAD51 (PDB:5NP7) on single-stranded DNA and the Henderson-Hasselbalch equation. (*C*) RAD51 foci formation was decreased in DT40 cells harboring RAD51 C319S protein following IR with 5 Gy. IF images of RAD51 DT40 cells transduced with WT or cysteine mutant RAD51 expression constructs processed 4 h following IR with 5 Gy. Scale bar 10 μm.

Supplemental Figure S2. Cys319Ser RAD51 cells exhibit diminished proliferation and CRISPR C319S RAD51 cells have smaller colonies in soft agar

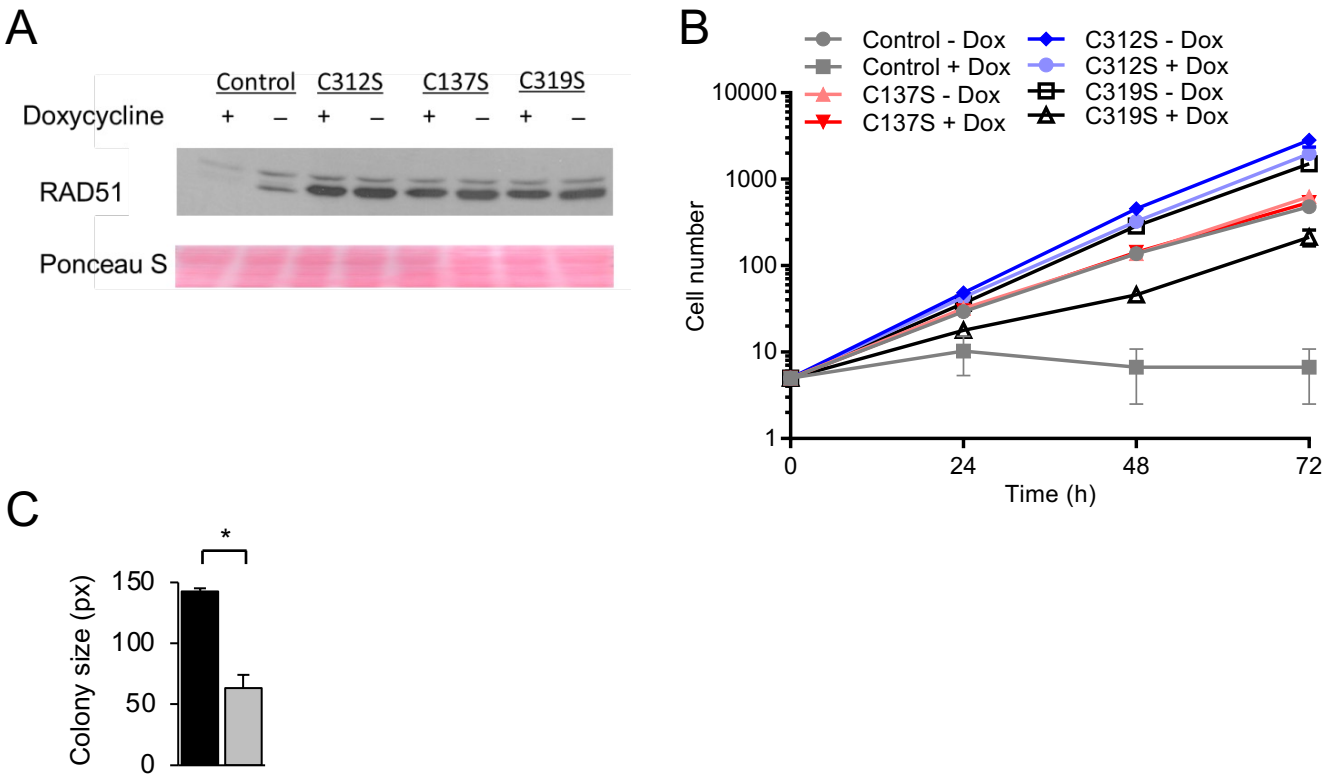

Supplemental Figure S2. Cys319Ser RAD51 cells exhibit diminished proliferation and CRISPR C319S RAD51 cells have smaller colonies in soft agar. (*A*) Expression of RAD51 protein in Tet-off RAD51 DT40 cells is indicated for RAD51 mutants. (*B*) Dox-dependent knockdown of RAD51 in DT40 cells suppressed proliferation in control Tet-repressed DT40 cells (●) and DT40 cells harboring human RAD51 C319S (Δ), but not DT40 cells transduced with RAD51 C137S (▼) or C312S (●) mutant expression constructs. Raw cell number counts are indicated over 72 h. (*C*) Soft agar colony formation assays were performed of RAD51 WT MM231 or CRISPR/Cas-9 homozygous Cys319Ser RAD51 mutated cells by plating 1000 cells in soft agar and measuring colony size after 4 weeks. Values indicate mean ± SEM, n=3.

Supplemental Figure S3. No disulfide between PRDX1 and RAD51 was detected and loss PRDX1 increases RAD51 sulfenylation

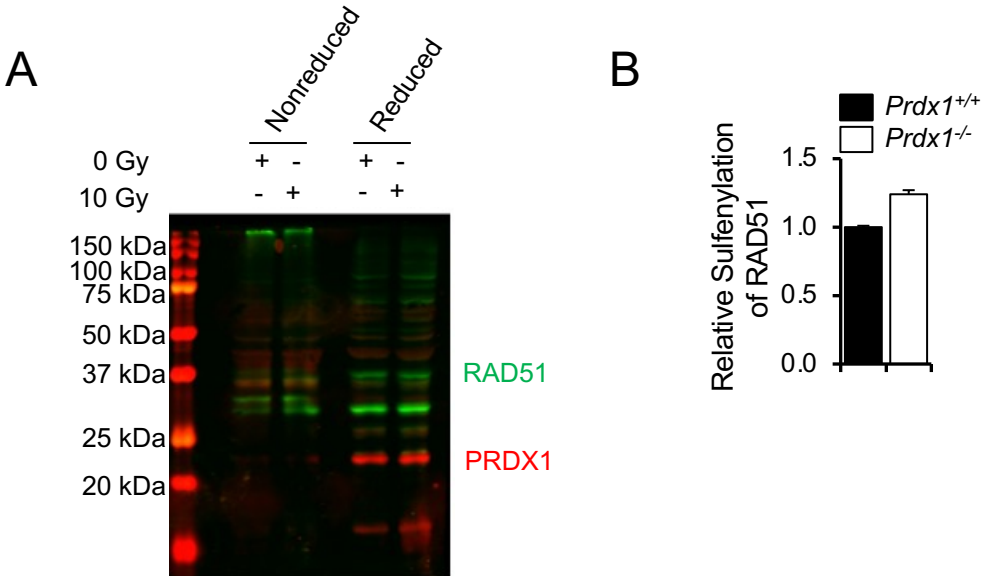

Supplemental Figure S3. (*A*) MCF10A cells were treated with 0 or 10 Gy and formation and separated under nonreducing or reducing conditions and immunoblotted for PRDX1 and RAD51. No disulfide bond was observed following irradiation. *(B) Prdx1*$^{-/-}$ MEFs were found to have increased levels of sulfenylated RAD51 relative to *Prdx1*$^{+/+}$ MEFs as measured by DAz-2 incorporation. MEFs were transduced with a RAD51 expression construct and treated with DAz-2 (5 mM) for 1.5 h. DAz-2 incorporation was detected by chemiluminescence by utilizing ligation of p-biotin and binding of streptavidin-HRP.

Supplemental Figure S4. PRDX1-deficiency sensitizes cells to IR and inhibits both HR and RAD51 foci formation

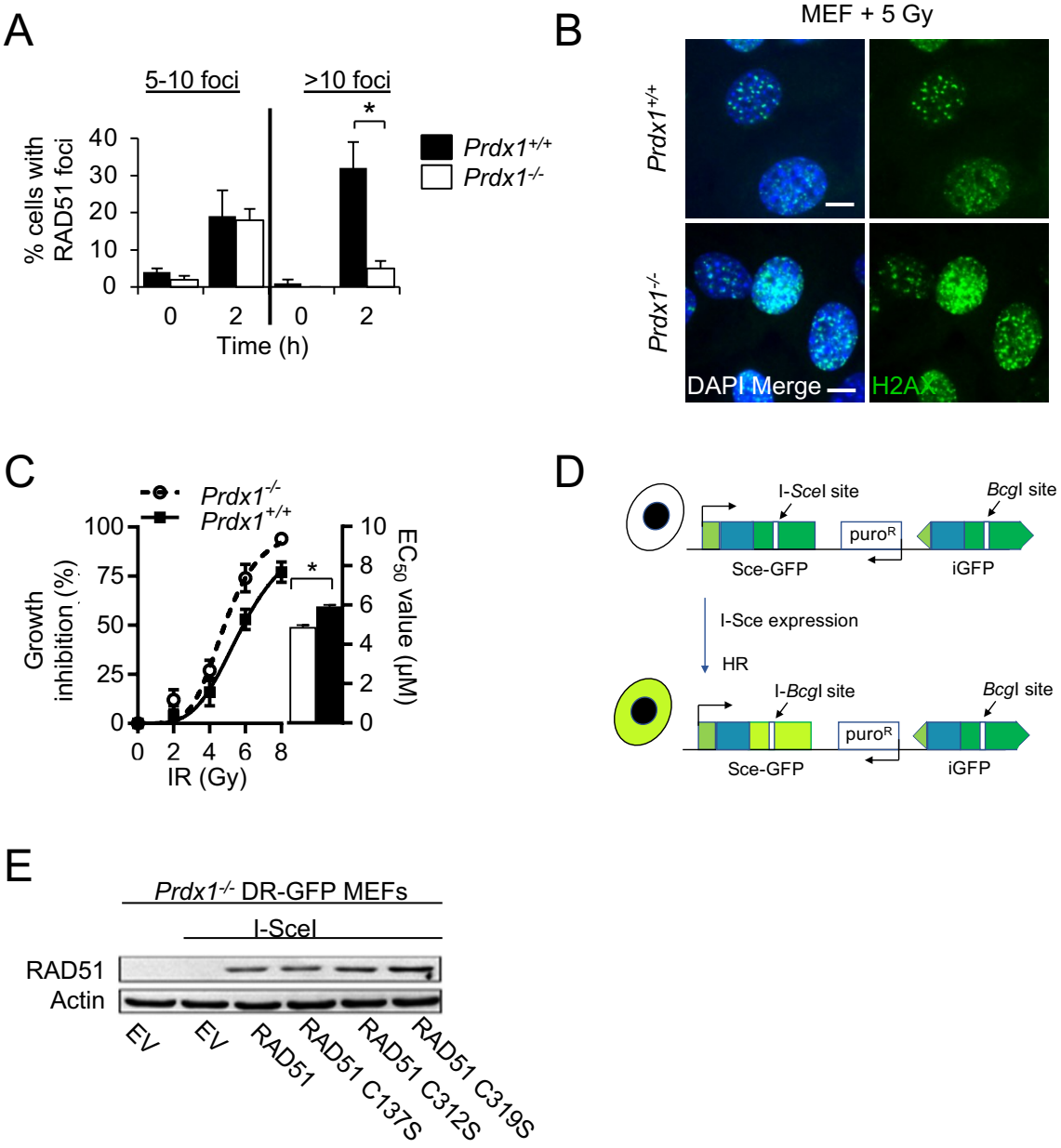

Supplemental Figure S4. PRDX1-deficiency sensitizes cells to IR and inhibits both HR and RAD51 foci formation. (*A*) PRDX1 deficiency decreased RAD51 foci formation when challenged with IR. *Prdx1*$^{+/+}$ (black bars) or *Prdx1*$^{-/-}$ (white bars) MEFs underwent IR with 0 or 5 Gy and RAD51 foci were counted after 2 h. RAD51 foci were binned into 5-10 foci or >10 foci. (*B*) PRDX1 deficiency increased γH2AX when irradiated with 5 Gy. IF images of *Prdx1*$^{+/+}$ or *Prdx1*$^{-/-}$ MEFs stained with γH2AX antibody post-IR with 5 Gy. Scale bar indicates 10 μm. (*C*) *Prdx1*$^{-/-}$ MEFs are more sensitive to IR when compared to *Prdx1*$^{+/+}$ MEFs. Clonogenic growth inhibition was measured in *Prdx1*$^{+/+}$ (■) or *Prdx1*$^{-/-}$ (○) MEFs following increasing doses of γ-IR. (*D*) DR-GFP assay for homologous-directed recombination of a modified tandem GFP reporter, which contains two differently mutated GFP cDNA fragments. Transient I-SceI expression initiates a DSB at the GFP I-SceI site. Repair of the DSB by a non-crossover gene conversion downstream of the second GFP cDNA fragment results in reconstitution of a functional GFP coding sequence with loss of the I-SceI site and gain of a BcgI site. (*E*) HR was decreased in *Prdx1*$^{-/-}$ MEFs harboring a DR-GFP reporter that expressed RAD51 C319S protein following DSB induced by I-SceI. Relative protein levels are indicated of *Prdx1*$^{-/-}$ MEFs transduced with WT or cysteine mutant RAD51 expression constructs transfected with I-SceI.

Supplemental Figure S5. PRDX1-deficiency sensitizes breast cancer cells to IR and diminishes RAD51 foci intensity

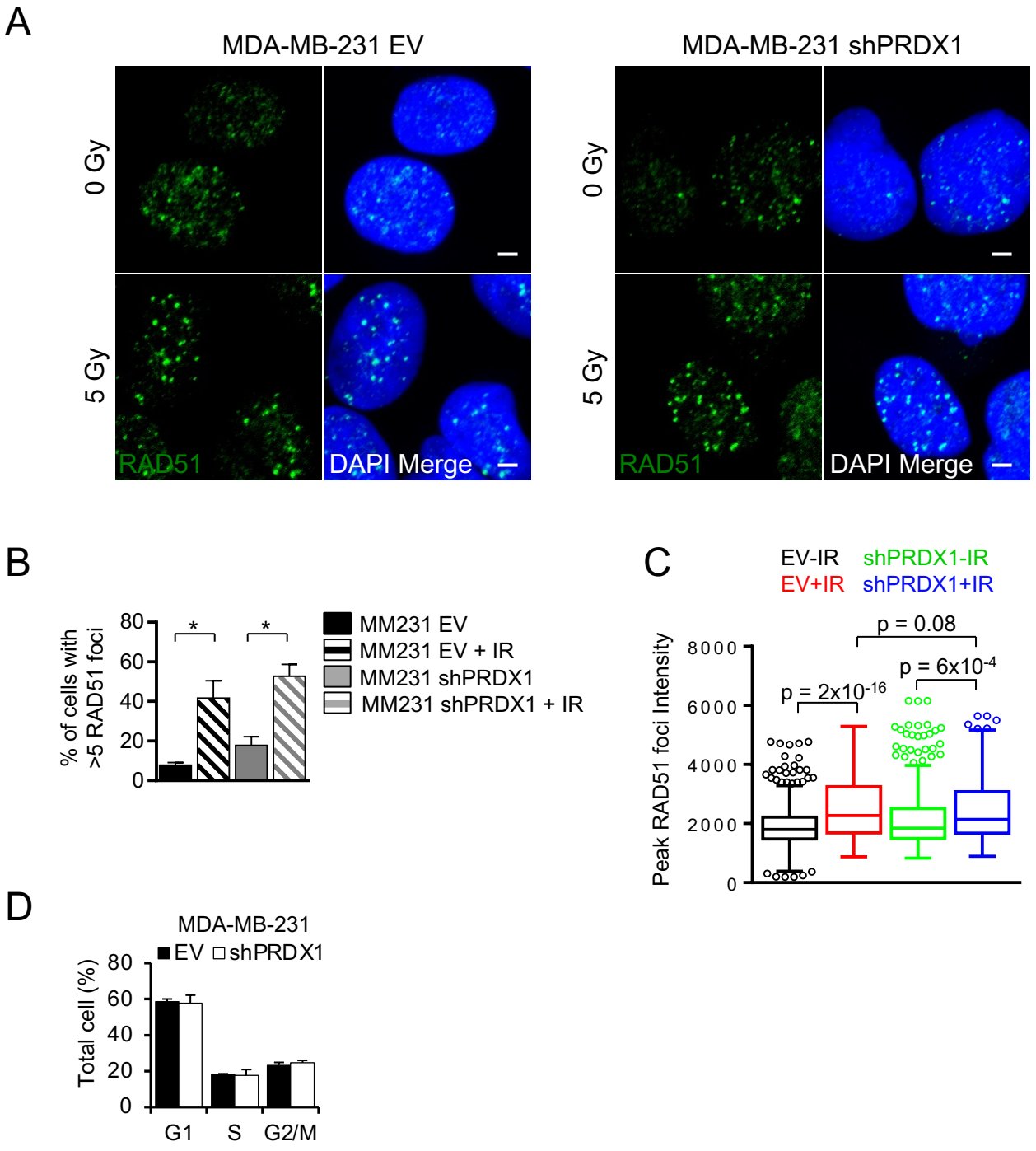

Supplemental Figure S5. PRDX1-deficiency sensitizes breast cancer cells to IR and diminishes RAD51 foci intensity. (*A*) MDA-MB-231 infected with shPRDX1 or EV expression vectors dosed with 0 or 5 Gy. Cells plated on 16-well coverslips were dosed with 0 or 5 Gy then processed for IF 6 hours later. Representative IF images are shown. Pseudo-coloring of RAD51 (green) and merged samples include DAPI stained nuclei (blue). Scale bar indicates 5 μm. (*B*) The mean percentages of cells with 5 or more RAD51 foci from confocal z-stacked images are indicated from PRDX1-proficient (black) or deficient (gray) samples following treatment with 0 (solid) or 5 Gy (striped) + SEM. (*C*) Box and whiskers plot of peak RAD51 foci intensity values of PRDX1-deficient (— or —) or proficient (— or —) MDA-MB-231 cells in the presence or absence of 5 Gy from more than 20 cells per group. (*D*) Flow cytometric analysis of propidium iodide stained breast cancer cells that were proficient or deficient in PRDX1 displayed a similar cell cycle profile. Mean ± SEM, n=3

Supplemental Table S1.

MDA-MB-231	p-value
EV vs. shPRDX1	0.627
EV vs. EV + IR	$< 2.2 \times 10^{-16}$
shPRDX1 vs. shPRDX1 + IR	0.000583
EV + IR vs. shPRDX1 + IR	0.084

Supplemental Table S1. IR enhanced RAD51 peak foci intensity more significantly in MDA-MB-231 EV cells compared to MDA-MB-231 shPRDX1 cells. MDA-MB-231 EV or MDA-MB-231 shPRDX1 cells were plated on coverslips and dosed with 0 or 5 Gy then processed for IF 6 hours later. RAD51 peak foci intensities from confocal z-stacked images from more than 20 cells per group were measured with MATLAB from 3 independent experiments. IR enhanced RAD51 peak foci intensity more significantly in MM231 EV cells compared to MDA-MB-231 shPRDX1 cells.